Sequential Ligation of Mg^+, Fe^+, (c-C_5H_5)Mg^+, and (c-C_5H_5)Fe^+ with Ammonia in the Gas Phase: Transition from Coordination to Solvation in the Sequential Ligation of Mg^+

Rebecca K. Milburn, Vladimir I. Baranov, Alan C. Hopkinson, and Diethard K. Bohme*

Department of Chemistry and Centre for Research in Earth and Space Science, York University, Toronto, Ontario, Canada, M3J 1P3

Received: April 17, 1998; In Final Form: September 14, 1998

Experimental results are reported that track the kinetics of the sequential ligation of Mg^+, Fe^+, (c-C_5H_5)Mg^+, and (c-C_5H_5)Fe^+ with ammonia in the gas phase as a function of the number of ligands added. The energetics of the sequential ligation of Mg^+ with ammonia has also been followed theoretically. Molecular orbital calculations with density functional theory (DFT) performed at the B3LYP/6-31+G(d) level have been used to compute the binding energies for direct coordination of the ammonia molecules with Mg^+ and for solvation that involves N−H···N interactions. Single-point calculations were also done using the optimized geometries from B3LYP/6-31+G(d) at B3LYP/6-311++G(2df,p) and MP4SDTQ(fc)/6-311++G(2df,p). Relative binding energies and standard enthalpies of formation ($\Delta H°_{f,298}$) have been calculated at all three levels of theory investigated. The experiments were performed with a selected-ion flow tube (SIFT) apparatus in helium buffer gas at 0.35 ± 0.01 Torr and 294 ± 3 K. The measured rate coefficients for ligation of both atomic metal ions exhibit a maximum for the second addition of ammonia, which disappears in the presence of a c-C_5H_5 substituent as the rate of ligation of Mg^+ and Fe^+ is enhanced by about 2 orders of magnitude. These trends have been interpreted in terms of the dependence of the lifetime of the collision intermediate on its degrees of freedom and the depth of its potential energy well. For the ligation of Mg^+, we propose that the precipitous drop in the observed rate of ligation of the fourth ligand and the emergence of a weakly bonded population of ligated ions in measured multicollision-induced dissociation spectra for $Mg(NH_3)_3^+$ and $Mg(NH_3)_4^+$ may signify *a change in the nature of the bonding* from direct bonding to hydrogen bonding in a second coordination shell with the addition of the third ligand. The observed variations in onset energy for multicollision-induced dissociation generally are consistent with a negative trend in the ligation energy with increasing ligation for the four ligated systems investigated.

Introduction

Great strides have been made in the past several years in characterizing *intrinsic* features of the ligation of metal ions through a large range of gas-phase measurements and ab initio molecular orbital calculations.[1] Progress has been such that the *sequential* ligation of metal ions M^+ now can be tracked in the gas phase through measurements of rate coefficients for reactions of type 1 as a function of the number of added ligand molecules L, where S is a third molecule that serves to collisionally stabilize the ligated ion ML_{n+1}^+.

$$ML_n^+ + L + S \rightarrow ML_{n+1}^+ + S \qquad (1)$$

For example, we have recently reported such measurements for the sequential ligation of Fe^+ with a variety of inorganic and organic ligands using a double mass spectrometer flow system operating at *room temperature* and at a helium buffer gas pressure (S = He) sufficiently high to allow collisional stabilization of the ligated ions ML_{n+1}^+.[2] Measurements such as these provide insight into the intrinsic efficiency of ligation and provide a kinetic measure of intrinsic coordination numbers for metal ions.[2a,d] Coordination numbers are accessible because rate coefficients for ligation are sensitive to the bond energies of the ligated ions, $D(ML_n^+\text{-L})$. This is so, since *gas-phase* ligation at moderate pressures proceeds in two steps: the formation of a transient intermediate, reaction 2, and collisional stabilization, reaction 3.

$$ML_n^+ + L \rightleftarrows (ML_{n+1}^+)^* \qquad (2)$$

$$(ML_{n+1}^+)^* + He \rightarrow ML_{n+1}^+ \qquad (3)$$

The lifetime of the transient intermediate $(ML_{n+1}^+)^*$ against dissociation back to reactants is dependent both on the degrees of freedom effective in intramolecular energy redisposition in the transient intermediate $(ML_{n+1}^+)^*$ and on its attractive well depth, $D(ML_n^+\text{-L})$, viz. the ligation energy of ML_n^+.[3]

Here, we report measurements of the intrinsic ligation kinetics for the ligation of Mg^+ and Fe^+ with ammonia. In principle, two types of ligation can occur when more than one ammonia molecule adds to a cation; either the ammonia can bond directly to the core ion ("inner-shell" ligation) or it may bond to an existing ammonia ligand by weak hydrogen bonding ("outer-shell" ligation). For example, we have suggested previously that both types of bonding occur in highly ligated $FeO(H_2O)_n^+$ and that measured rate coefficients for sequential ligation reveal a transition between the two types of ligation at $n = 3$.[2a] Here, we explore such a transition more closely by comparing measured rates in the ligation of Mg^+ with ammonia with ligation energies calculated for both direct bonding with Mg^+

10.1021/jp981914z CCC: $15.00
Published on Web 11/04/1998

and hydrogen bonding with an existing ammonia ligand using standard ab initio molecular orbital theory. Computed ammonia-ligation energies for direct bonding have been reported previously by Bauschlicher and co-workers.[4,5] The observed kinetics for sequential ligation of Fe^+ with ammonia is compared with experimentally[6,7] and theoretically[8] determined ligation energies for addition of up to four ammonia molecules. Also, after their formation, the ligated ions ML_n^+ are subjected to collision-induced dissociation in experiments designed to ascertain insights into the structures of the ligated ions and into relative binding energies. Again, our aim here is to ascertain whether a transition between the two types of ligation is revealed in measured rate coefficients for sequential ligation and whether "outer-shell ligation" can be shown to proceed before "inner-shell" ligation is complete. Evidence for the latter has recently been reported by Weinheimer and Lisy for methanol solvation of Cs^+ using vibrational spectroscopy.[9]

Also, we extend the intrinsic ligation studies to "heterogeneous" ligation. The kinetics of sequential ligation of the metal ion already ligated with another ligand $L' = c\text{-}C_5H_5$ is tracked as a function of the number of added ligands $L = NH_3$. The generalized ligation is illustrated in reaction 4.

$$L'ML_n^+ + L + He \rightarrow L'ML_{n+1}^+ + He \qquad (4)$$

Such studies provide an opportunity to examine the role of degrees of freedom in the transient intermediate on the measured coefficient of the rate of ligation. Again, after their formation, the ligated ions $L'ML_n^+$ are subjected to collision-induced dissociation to ascertain insights into the structures of the ligated ions and relative binding energies and also to probe for the occurrence of intramolecular ligand−ligand interactions.

Experimental Methods

Experiments were performed using a selected ion flow tube (SIFT) apparatus.[10] The ions Mg^+, Fe^+, $(c\text{-}C_5H_5)Mg^+$, and $(c\text{-}C_5H_5)Fe^+$ were produced in a low-pressure ion source by electron-impact dissociative ionization of magnesocene or ferrocene vapor at electron energies between 35 and 50 eV. The ions produced in the source were mass-selected through a quadrupole mass filter, introduced into the flow tube via a Venturi aspirator, and allowed to thermalize by collisions (about 4×10^5) with helium buffer gas before entering the reaction region further downstream. At the end of the reaction region all ions were sampled by a second quadrupole mass filter. The neutral reactant, ammonia, was anhydrous grade, with a minimum purity of 99.99%, supplied by Matheson Gas Products. Rate coefficients and product distributions were measured in the usual manner.[10] All measurements were performed at a room temperature of 294 ± 3 K and at a helium operating pressure of 0.35 ± 0.01 Torr. Bond connectivities in the product ions were probed with multicollision-induced dissociation (CID) experiments as described previously by raising the sampling nose-cone voltage from 0 to −80 V without introducing mass discrimination.[11] The observed dissociation threshold for a particular ion is determined from the intercept of the baseline with the fastest-growing portion of the appearance curve for the product ion. The quantitative interpretation of the measured thresholds in terms of absolute binding energies is problematic, since the theory of multicollision-induced dissociation is not completely understood.[11] Consequently, the CID measurements are used primarily to ascertain bond connectivities and to provide insight into relative binding energies.

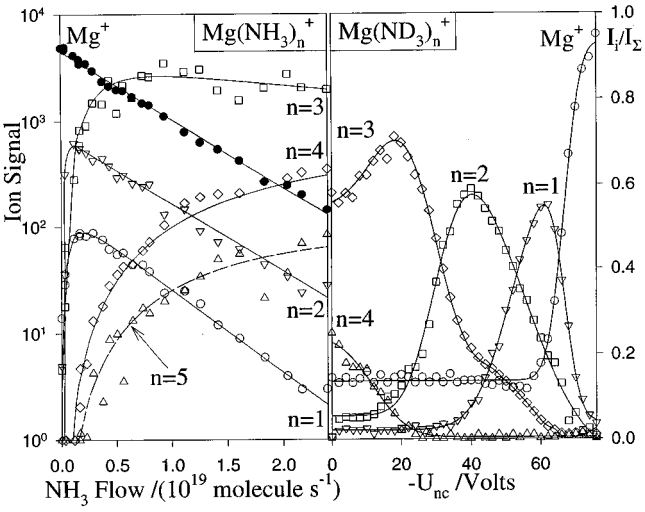

Figure 1. (Left) Experimental data recorded for the reaction of Mg^+ with ammonia in helium buffer gas at 294 ± 3 K and 0.35 ± 0.01 Torr. The Mg^+ ions were produced in a low-pressure ion source by electron impact dissociative ionization of magnesocene vapor at 35 eV. The solid lines represent a fit to the experimental data with the solution to the differential equations appropriate for the sequential addition reactions. Rate coefficients derived from the fit are given in Table 1. (Right) Results of multicollision CID experiments. The flow of deuterated ammonia is 2.0×10^{19} molecules s^{-1}.

Computational Methods

Standard ab initio molecular orbital calculations were performed using the GAUSSIAN 94 program.[12] The density functional Becke three-parameter hybrid method[13] that includes the Slater (local spin density) exchange functional[13a,b,14] with nonlocal gradient-corrected terms included[15] and the Lee−Yang−Parr method, which includes local and nonlocal gradient-corrected correlation functionals, was used to optimize geometries.[16,17] Use of this method with a basis set of 6-31+G(d) will be denoted B3LYP/6-31+G(d). The optimized geometries at B3LYP/6-31+G(d) were characterized by harmonic frequency calculations, and these showed all structures to be at minima. The frequency calculations also yielded both zero-point energies, which are unscaled, and thermal corrections for all the ions. Single-point calculations were done using density functional theory with a basis set of 6-311++G(2df,p) using optimized geometries from B3LYP/6-31+G(d). Single-point calculations were also done at fourth-order Møller−Plesset[18] theory with a frozen core, again using the basis set 6-311++G-(2df, p) with geometries from B3LYP/6-31+G(d) optimizations.

Experimental Results

Ligation of Mg^+ and Fe^+ with Ammonia. Up to five molecules of ammonia were observed to add to Mg^+ in reactions of type 5 and three molecules of ammonia sequentially ligated Fe^+ in reactions of type 6.

$$Mg(NH_3)_n^+ + NH_3 \rightarrow Mg(NH_3)_{n+1}^+ \qquad (5)$$

$$Fe(NH_3)_n^+ + NH_3 \rightarrow Fe(NH_3)_{n+1}^+ \qquad (6)$$

Experimental ligation and ligand-dissociation profiles are shown in Figures 1 and 2. The measured rate coefficients for sequential ligation reactions 5 and 6 are summarized in Table 1 along with calculated collision rate coefficients.[19] Rate coefficients for the ammonia ligation of $Mg(NH_3)_4^+$ and $Mg(NH_3)_5^+$ could not be

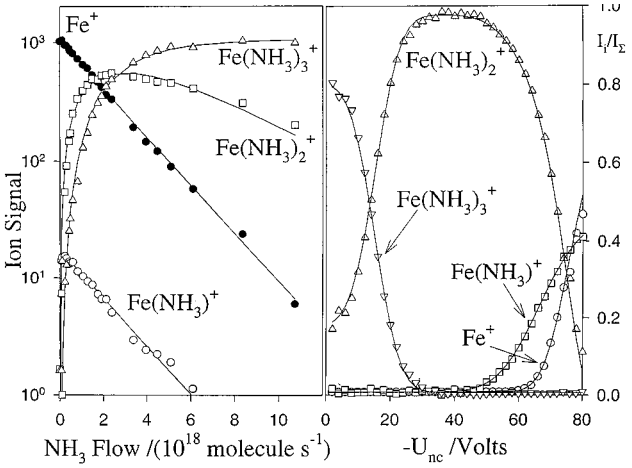

Figure 2. (Left) Experimental data recorded for the reaction of Fe^+ with ammonia in helium buffer gas at 294 ± 3 K and 0.35 ± 0.01 Torr. The Fe^+ ions were produced in a low-pressure ion source by electron impact dissociative ionization of ferrocene vapor at 35 eV. The solid lines represent a fit to the experimental data with the solution to the differential equations appropriate for the sequential addition reactions. Rate coefficients derived from the fit are given in Table 1. (Right) Results of multicollision CID experiments. The flow of ammonia is 1.3×10^{19} molecules s^{-1}.

TABLE 1: Effective Bimolecular Rate Coefficients (in Units of cm^3 molecules^{-1} s^{-1}) for the Ligation Reactions of Mg^+ and Fe^+ with *n* Molecules of Ammonia at 294 ± 3 K in Helium Buffer Gas and at a Total Pressure of 0.35 ± 0.01 Torr

ion	*n*	k_{obs}[a]	k_c[b]
Mg^+	0	$(4.1 \pm 1.2) \times 10^{-12}$	2.5×10^{-9}
	1	$(2.1 \pm 0.6) \times 10^{-10}$	2.3×10^{-9}
	2	$(5.5 \pm 1.7) \times 10^{-11}$	2.2×10^{-9}
	3	$(5.0 \pm 1.5) \times 10^{-13}$	2.1×10^{-9}
Fe^+	0	$(1.7 \pm 0.5) \times 10^{-11}$	2.2×10^{-9}
	1	$(1.0 \pm 0.3) \times 10^{-9}$	2.1×10^{-9}
	2	$(8.2 \pm 2.0) \times 10^{-12}$	2.1×10^{-9}
	3	$< 5 \times 10^{-14}$	2.0×10^{-9}

[a] The estimated maximum experimental uncertainty is given in parentheses. [b] Collision rate coefficient derived from the variational transition-state treatment of Su and Chesnavich.[19]

determined, since the profiles for these ions were not sufficiently developed to provide reliable rate coefficients by curve-fitting. The tabulated reaction rate coefficients are *effective bimolecular* rate coefficients. They were not investigated as a function of pressure because of the limited pressure range available with the SIFT technique, and so the molecularity of the ligation could not be determined experimentally. Nevertheless, reactions 1 and 2 almost certainly proceed by termolecular association under our experimental operating conditions (with He acting as the third body) rather than by bimolecular (radiative) association. It is interesting to note that ammonia was *not* found to cluster directly with Mg^+ in SIFT studies in which Mg^+ was produced in a glow discharge.[20]

A plot of the rate coefficient for ligation vs the number of ammonia molecules added is shown in Figure 3 for the sequential ammonia ligation of both Mg^+ and Fe^+. In both cases the rate of ligation increases for the singly ligated species and then drops sharply, and more so in the case of iron. The maximum rate of ligation is close to the collision limit, particularly in the case of Fe^+ ligation.

The multicollision CID profiles for Mg^+ ligated with deuterated ammonia observed at the relatively high ND_3 flow of 2.0×10^{19} molecules s^{-1} are shown in Figure 1. Deuterated

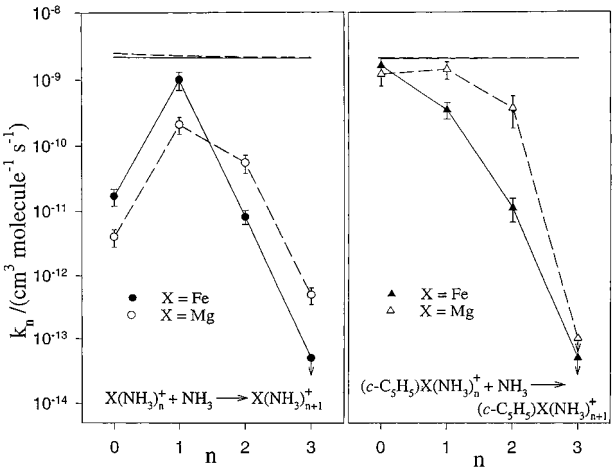

Figure 3. Variation of the effective bimolecular rate coefficient for the sequential ligation of Mg^+ and Fe^+ (left) and of $(c\text{-}C_5H_5)Mg^+$ and $(c\text{-}C_5H_5)Fe^+$ (right) with the number of ammonia ligands. The variations in the collision rate coefficients are indicated as straight lines and represent upper limits to the reaction rate coefficients.

ammonia was used to monitor any hydrogen loss, and none was observed. The CID profiles indicate the successive elimination of single ammonia molecules from $Mg(NH_3)_3^+$ and the elimination of one molecule of ammonia from $Mg(NH_3)_4^+$ to form $Mg(NH_3)_3^+$ at relatively low collision energies. Also, the inflection in the $Mg(NH_3)_3^+$ profile at ca. 40 V suggests the presence of two different states or isomers of $Mg(NH_3)_3^+$. The $Mg(NH_3)_5^+$ signal was too small for a measurement of its dissociation. A plausible interpretation of these results is that the first two and some of the third ammonia molecules are bonded strongly and that the fourth and most of the third molecules of ammonia are less strongly bound.

The onsets for dissociation in the multicollision CID profiles for $Fe(NH_3)_n^+$ shown in Figure 2 indicate a low stability against deligation for $Fe(NH_3)_3^+$ and a surprisingly high stability for $Fe(NH_3)_2^+$ against loss of ammonia. The onset for the dissociation of $Fe(NH_3)^+$ is masked by its dissociation almost immediately after its formation from $Fe(NH_3)_2^+$.

Ligation of $(c\text{-}C_5H_5)Mg^+$ and $(c\text{-}C_5H_5)Fe^+$ with Ammonia. Experimental ligation and ligand-dissociation profiles are shown in Figures 4 and 5. The measured rate coefficients for the sequential ligation reactions 7 and 8

$$(c\text{-}C_5H_5)Mg(NH_3)_n^+ + NH_3 \rightarrow (c\text{-}C_5H_5)Mg(NH_3)_{n+1}^+ \quad (7)$$

$$(c\text{-}C_5H_5)Fe(NH_3)_n^+ + NH_3 \rightarrow (c\text{-}C_5H_5)Fe(NH_3)_{n+1}^+ \quad (8)$$

are summarized in Table 2 along with calculated collision rate coefficients. The measured rate coefficients are again effective bimolecular rate coefficients, and reactions 7 and 8 also are likely to proceed by termolecular association with He acting as the third body. Up to three molecules of ammonia were observed to add sequentially to $(c\text{-}C_5H_5)Mg^+$ and to $(c\text{-}C_5H_5)Fe^+$.

A plot of the rate coefficient for ligation vs the number of ammonia molecules added is shown in Figure 3 for the sequential ammonia ligation of both $(c\text{-}C_5H_5)Mg^+$ and $(c\text{-}C_5H_5)Fe^+$. Both $(c\text{-}C_5H_5)Mg^+$ and $(c\text{-}C_5H_5)Fe^+$ are ligated rapidly, close to the collision rate, with one ammonia molecule. The rate of ligation increases only slightly for the addition of the second ammonia molecule to $(c\text{-}C_5H_5)Mg^+$, drops by less than a factor of 10 for the addition of the third, and then becomes immeasurably small, $k < 1 \times 10^{-13}$ cm^3 molecule^{-1} s^{-1}, for

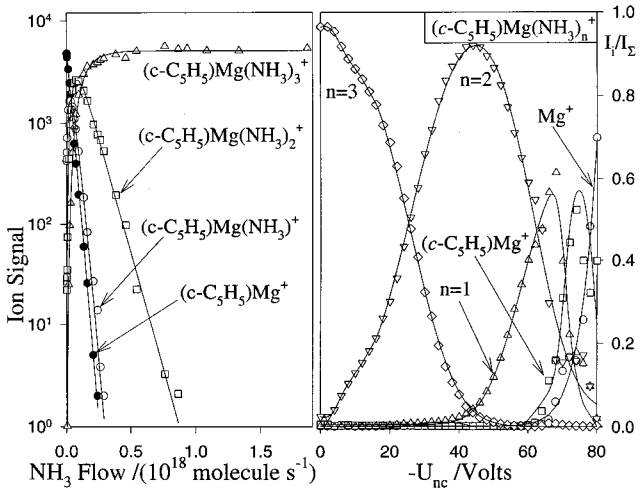

Figure 4. (Left) Experimental data recorded for the reaction of (*c*-C_5H_5)Mg^+ with ammonia in helium buffer gas at 294 ± 3 K and 0.35 ± 0.01 Torr. The (*c*-C_5H_5)Mg^+ ions were produced in a low-pressure ion source by electron impact dissociative ionization of magnesocene vapor at 50 eV. The solid lines represent a fit to the experimental data with the solution to the differential equations appropriate for the sequential addition reactions. Rate coefficients derived from the fit are given in Table 1. (Right) Results of multicollision CID experiments. The flow of ammonia is 1.0×10^{18} molecules s^{-1}.

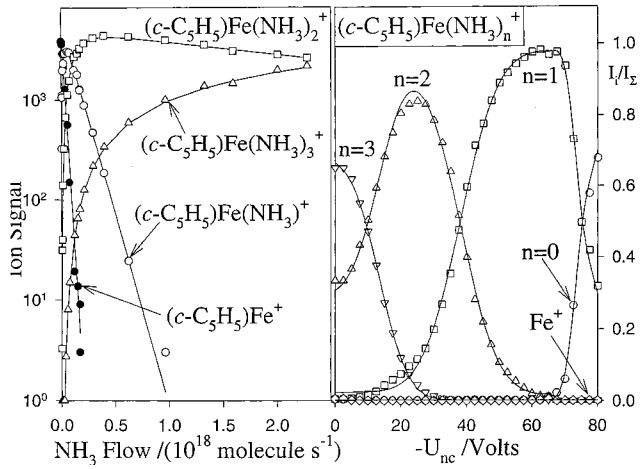

Figure 5. (Left) Experimental data recorded for the reaction of (*c*-C_5H_5)Fe^+ with ammonia in helium buffer gas at 294 ± 3 K and 0.35 ± 0.01 Torr. The (*c*-C_5H_5)Fe^+ ions were produced in a low-pressure ion source by electron impact dissociative ionization of ferrocene vapor at 50 eV. The solid lines represent a fit to the experimental data with the solution to the differential equations appropriate for the sequential addition reactions. Rate coefficients derived from the fit are given in Table 1. (Right) Results of multicollision CID experiments. The flow of ammonia is 3.0×10^{18} molecules s^{-1}.

the addition of another ammonia molecule. The rate of ligation of (*c*-C_5H_5)Fe^+ already drops on addition of the second ammonia molecule, continues to drop for higher additions, and becomes immeasurably small for the addition of the fourth ammonia molecule.

Theoretical Results

Optimized structures computed for $Mg(NH_3)_n^+$ ions with $n = 1-4$ are given in Figure 6, and their geometric parameters are listed in Table 3. For ions with $n > 1$, minima were found both for structures in which there is direct coordination of the ammonia molecule to the core magnesium atom and for "solvated" ion structures in which the "solvating" ammonia is hydrogen-bonded to one of the hydrogen atoms of a coordinating ammonia molecule (see Figure 6). The total electronic energies and zero-point energies (ZPE) for all of these ligated ions are given in Table 4.

TABLE 2: Effective Bimolecular Rate Coefficients (in Units of cm^3 $molecules^{-1}$ s^{-1}) for the Ligation Reactions of (*c*-C_5H_5)Mg^+ and to (*c*-C_5H_5)Fe^+ with *n* Molecules of Ammonia at 294 ± 3 K in Helium Buffer Gas and at a Total Pressure of 0.35 ± 0.01 Torr

	n	k_{obs}[a]	k_c[b]
(*c*-C_5H_5)Mg^+	0	$(1.2 \pm 0.4) \times 10^{-9}$	2.1×10^{-9}
	1	$(1.4 \pm 0.4) \times 10^{-10}$	2.0×10^{-9}
	2	$(3.7 \pm 1.9) \times 10^{-10}$	2.0×10^{-9}
	3	$<1 \times 10^{-13}$	2.0×10^{-9}
(*c*-C_5H_5)Fe	0	$(1.6 \pm 4.8) \times 10^{-9}$	2.0×10^{-9}
	1	$(3.5 \pm 1.0) \times 10^{-10}$	2.0×10^{-9}
	2	$(1.1 \pm 0.44) \times 10^{-11}$	2.0×10^{-9}
	3	$<5 \times 10^{-14}$	2.0×10^{-9}

[a] The estimated maximum experimental uncertainty is given in parentheses. [b] Collision rate coefficient derived from the variational transition-state treatment of Su and Chesnavich.[19]

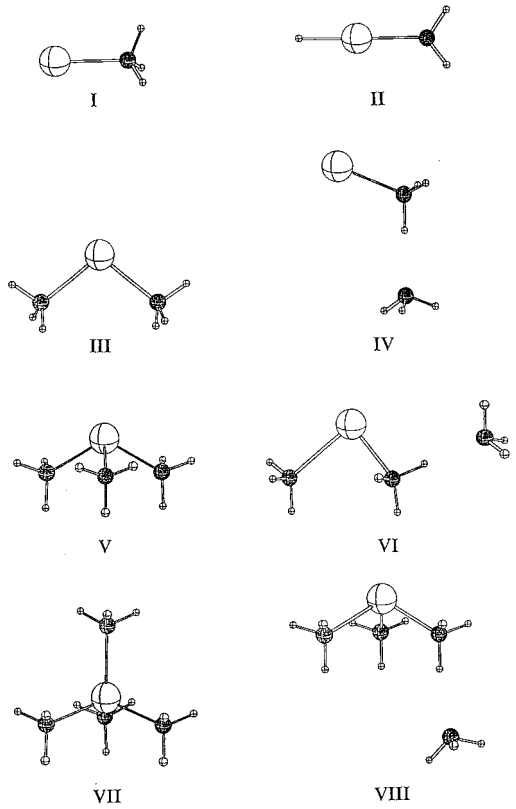

Figure 6. Optimized structures for the cations **I**−**VIII** at B3LYP/6-31+G(d). Bond lengths and angles are given in Table 6. Nitrogen atoms are represented with heavily shaded centers, magnesium atoms are represented with large unshaded centers, and hydrogen atoms are represented using small unshaded centers.

Two minima were found on the $MgNH_3^+$ surface: structures **I** and **II**. Structure **I**, where the bonding occurs through donation of the lone pair of electrons on nitrogen, is at the global minimum. Structure **II**, the insertion complex, is 51.0 kcal mol^{-1} above the global minimum at B3LYP/6-31+G* (with ZPE included) and has an energy *higher* than that of the isolated reagents by 10.7 kcal mol^{-1}.

The Mg−N bond lengths in the directly coordinated $Mg(NH_3)_n^+$ ions increase as the number of ammonia adducts increases from 2.193 Å (for $n = 1$) to 2.229 Å (for $n = 3$). This trend is reversed for the quadruply ligated tetrahedral Mg-

TABLE 3: Optimized Structures for the Cations I−VIII at B3LYP/6-31+G(d), Bond Lengths (Å), and Bond Angles (deg)[a]

structure (symmetry)	MgN	∠MgNH	∠NMgN	N···H
I (C_{3v})	2.193	113.1		
II[b] (C_{2v})	2.147	126.4		
III (C_{2v})	2.218	109.4 (2H)	103.0	
		115.1 (4H)		
IV (C_s)	2.138	112.5 (1H)		1.880
		113.1 (2H)		
V (C_{3v})	2.229	109.8 (6H)	100.5	
		119.6 (3H)		
VI (C_1)	2.224	109.6 (2H)	103.1	1.913
	2.165	114.8 (4H)		
VII (T_d)	2.156	113.1 (12H)	109.5	
VIII (C_1)	2.229	110.0 (6H)	100.9	2.024
	2.191	119.3 (3H)		

[a] N−H distances in the ligated NH_3 vary from 1.021 to 1.030 Å (in free NH_3 the distance is 1.021 Å). When the H is H-bonded to a solvating NH_3 molecule, the N−H varies from 1.041 to 1.057 Å. [b] The Mg−H distance is 1.667 Å; ∠NMgH = 180.0°.

$(NH_3)_4^+$ in which the Mg−N bond length is the shortest at 2.156 Å. Structure **III**, $Mg(NH_3)_2^+$, has an NMgN bond angle of 103.0°, consistent with the value of 99.9° at SCF/TZ2P reported by Bauschlicher and co-workers.[4] This angle is much smaller than expected, since the unpaired electron is formally located on the magnesium. According to these authors, the second ammonia ligand does not bond on the opposite side of the magnesium from the first ligand because this is a region of high electron density; the magnesium 3s orbital is polarized away from the first ligand to enhance the bonding between Mg^+ and the first ammonia. An alternative explanation is that bonding occurs through donation from nitrogen into the vacant p orbitals of magnesium, and the expected angle of 90° is increased slightly by steric interaction between the two ligands. This type of bonding, where the unpaired electron is essentially in the 3s orbital, can be attributed to the larger s−p gap that occurs in the second full row of the periodic table. This type of bonding would also lead to the three-coordinate ion having small NMgN angles, and the angles in ion **V** are indeed slightly smaller than in diadduct **III**. In $Mg(NH_3)_4^+$ there are formally nine valence electrons around the magnesium atom, eight from lone pairs donated from the four ammonia molecules, and the ninth originating from Mg^+. However, the complex does not adopt either a trigonal-bypyramidal or a square-pyramidal structure. Rather, it prefers a tetrahedral arrangement. The unpaired electron is in an orbital of a_1 symmetry to which the major contributor is the outer s function on the magnesium. In terms of atomic orbitals on magnesium, this corresponds to the magnesium accepting electrons (from the nitrogen atoms) into sp^3 hybrid orbitals constructed from the 3s and 3p orbitals and the unpaired electron being in the 4s orbital.

Structures **IV**, **VI**, and **VIII** are solvated ions (see Figure 6). The N···H solvating distance is approximately twice that of the N−H bond distance in ammonia and increases as the number the ammonia molecules is increased. The directly coordinated core of the solvated complex, structure **VI**, has geometrical parameters similar to those of the unsolvated diadduct, structure **III**. Likewise, the directly coordinated core of the solvated ion **VIII** has structural parameters similar to those of **V**. The geometries of the solvating NH_3 molecules in the solvated ions **IV**, **VI**, and **VIII** have dimensions comparable to those of an isolated ammonia molecule. All these structural parameters indicate relatively small interactions between ions and a solvating ammonia molecule.

Binding enthalpies for the directly bonded and the solvated $Mg(NH_3)_n^+$, $n = 1-4$, are given in Table 5 at all three levels of theory. Our value for the Mg^+-NH_3 binding enthalpy in the first adduct, 39.7 kcal mol^{-1} at both B3LYP/6-311++G-(2df,p) and MP4SDTQ(fc)/6-311++(2df,p), is in agreement with the values of 38.7 ± 5 and 40.0 kcal mol^{-1} calculated by Bauschlicher et al.[4,5] As the number of ammonia ligands increases, the binding enthalpies of the directly bonded ions as calculated at B3LYP/6-31+G(d) decrease from 41.4 kcal mol^{-1} for $Mg(NH_3)^+$ to 15.5 kcal mol^{-1} for $Mg(NH_3)_4^+$. The calculated binding enthalpies for the solvated ions are always smaller than those for the directly bonded ions. They also decrease with the number of bonded ammonia molecules and range between 16.0 and 10.4 kcal mol^{-1}. However, it is interesting to note that the difference between the bond enthalpies of ions containing directly bonded ammonia molecules and those of their solvated isomers steadily decreases with increasing ligation. This is evident from Figure 7.

For structures **I**, **III**, **V**, and **VII**, three levels of theory were used to calculate the standard enthalpies of formation at 298 K. The results are summarized in Table 6. It has been shown previously that enthalpies of formation obtained at MP4SDTQ-(fc)/6-311++G(2df,p) are within ±2 kcal mol^{-1} of experimental values.[21,22] The single-point DFT calculations at B3LYP/6-311++G(2df,p) yield values of comparable accuracy that are lower than the MP4 enthalpies by at most 1.4 kcal mol^{-1} for structures **I** and **III**. Calculations for the larger structures **V** and **VII** were restricted to DFT calculations with the 6-31+G* basis set. We estimate that the error in these enthalpies of formation is likely to be ±10 kcal mol^{-1}. There are no current literature values available for the standard enthalpies of formation of these four ions, either theoretical or experimental.

Discussion

Our gas-phase measurements have allowed us to track both the kinetics and the energetics of sequential ligation as a function of the number of ligands added. For the ligation of Mg^+ and Fe^+ with ammonia, the measured rate coefficients show a dramatic increase in the rate of ligation after the addition of the first ammonia ligand followed by a fairly rapid decrease in rate (see Figure 3). The *c*-C_5H_5 ligand dramatically enhances the rate of ligation of the first ammonia ligand, but a drop in rate is again observed for higher degrees of ammonia ligation (see Figure 3). We can qualitatively account for these rate enhancements and profiles in terms of the classical two-step ligation mechanism indicated by reactions 2 and 3. This mechanism predicts a rate coefficient directly proportional to the lifetime of the transient intermediate $(ML_{n+1}^+)^*$ given by expression 9 for nonlinear intermediates,

$$\tau = A\{(D + 3RT)/(3RT)\}^{(s-1)} \quad (9)$$

where A is a time corresponding to the period of one vibration.[23] It is seen that this lifetime is determined by the attractive well depth, $D(ML_n^+\text{-L})$, and the degrees of freedom, s, effective in the redisposition of the excess energy of the activated intermediate. As a consequence, the rate coeffcient for ligation can be expected to increase with increasing binding energy of ligation and increasing molecular complexity of the ligand.

Thus, the addition of the first ammonia is slow because the effective degrees of freedom, the binding enthalpy of the intermediate, or both are relatively small. The addition rate of the second ammonia is about 100 times faster because the effective degrees of freedoms predominate in this addition and

TABLE 4: Computed Total Electronic Energies (in hartrees) and Zero-Point Energies (in kcal mol^{-1})

	total energies			
ion	B3LYP/ 6-31+G(d)	B3LYP/ 6-311++G(2df,p)[b]	MP4SDTQ(fc)/ 6-311++G(2df,p)[b]	ZPE[a]
I	−256.419 00	−256.457 33	−255.890 27	24.0
II	−256.328 45			17.5
$Mg^+ + NH_3$	−256.352 54	−256.709 68	−255.826 44	21.7
III	−313.025 86	−313.088 21	−312.402 83	48.0
IV	−313.003 91			47.7
I + NH_3	−312.975 99	−313.041 66	−312.352 82	45.7
V	−369.622 98	−369.709 68		70.1
VI	−369.607 03			71.6
III + NH_3	−369.582 85	−369.672 54	−368.865 38	69.7
VII	−426.205 90			94.0
VIII	−426.199 97			95.6
V + NH_3	−426.179 97	−426.294 01		91.8
Mg^+	−199.795 55	−199.809 28	−199.363 89	0.0
NH_3	−56.556 99	−56.584 33	−56.462 55	21.7

[a] Unscaled zero-point energies at B3LYP/6-31+G(d). [b] Single-point calculations.

TABLE 5: Calculated Binding Enthalpies (in kcal mol^{-1}) at 298 K

	binding enthalpies			
ion	B3LYP/ 6-31+G(d)	B3LYP/ 6-311++ G(2df,p)	MP4SDTQ(fc)/ 6-311++ G(2df,p)	other theoretical results[a]
I	41.4	39.7	39.7	38.7 ± 5,[b] 40.0[c]
III	30.3	28.2	30.4	31.4[c]
IV	16.0			
V	26.2	22.3		26.2[c]
VI	13.7			
VII	15.5			
VIII	10.4			

[a] Binding energies at 0 K have been revised to bond enthalpies at 298 K. [b] At MCPF(ANO); ref 5. [c] At SCF(TZP); ref 4.

increase the rate even though, in the case of Mg^+ ligation, the binding enthalpy of the second ligand is smaller than that of the first. In the case of Fe^+ ligation the binding enthalpy actually increases for the addition of the second ammonia molecule, and this would be expected to enhance the rate of formation of the doubly ligated species even further. Figure 3 shows that formation of $Fe(NH_3)_2^+$ occurs at the collision limit. The rate of ligation of the third ammonia molecule decreases slightly in the case of magnesium and by a factor of more than 100 in the case of iron, even though the effective degrees of freedom are likely to *increase*. A further drop in the measured rate coefficient by a factor of almost 100 in the case of magnesium and more than 100 in the case of iron is observed for the addition of the fourth ammonia molecule. The drop in the rate observed for these higher degrees of ligation presumably signifies a controlling influence of the decreasing binding enthalpy of ligation (see Figure 7) on the intermediate lifetime.

Bond enthalpies were not computed for the ammonia ligation of Fe^+, (c-C_5H_5)Mg^+, and (c-C_5H_5)Fe^+, but Figure 8 shows that the observed variations in onset energy for the removal of ligands by multicollision-induced dissociation generally are consistent with a negative trend in the ligation enthalpy with increasing ligation for all four ligated systems investigated. The one exception appears to be $Fe(NH_3)_2^+$ for which our CID measurements indicate an unusually high stability consistent with previous bond enthalpy measurements and calculations that show that the second ammonia molecule bonds more strongly than the others with $n = 1$, 3, and 4 (see Table 7). Thus, on the basis of the two-step ligation model, the general trend in the ligation rate coefficient with increasing ligation can be expected to be qualitatively similar for the ligation of all four

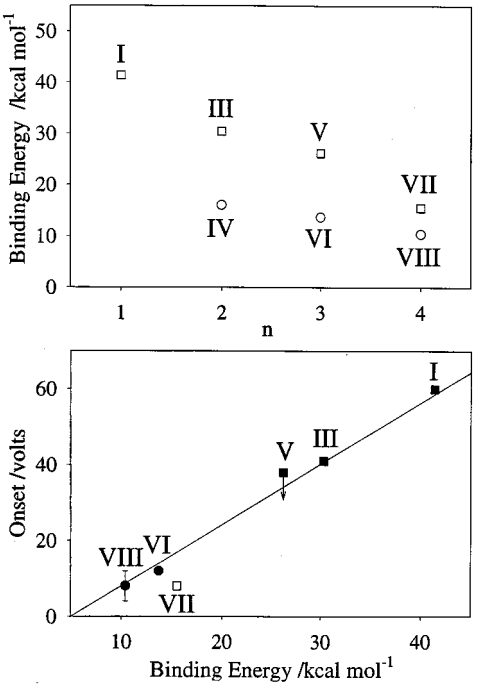

Figure 7. (Top) Computed variation in the binding enthalpy with the number of coordinatively bonded ammonia ligands for both directly bonded (**I**, **III**, **V**, **VII**) and hydrogen-bonded (**IV**, **VI**, **VIII**) ligation. (Bottom) Correlation of the measured onset voltage for multicollision-induced dissociation with calculated binding enthalpies for $Mg(NH_3)_n^+$. The onset voltages have been assigned an uncertainty of ±2 V except for the dissociation onset for $Mg(NH_3)_4^+$, which has an assigned uncertainty of ±4 V. The solid circles are attributed to solvated ions involving hydrogen bonding, and the solid squares are attributed to Mg^+ ligated ions. The open square, included for comparison only, is an unmeasured point with a calculated binding enthalpy for the direct ligation of the fourth ammonia molecule.

of the ions Mg^+, Fe^+, (c-C_5H_5)Mg^+, and (c-C_5H_5)Fe^+. The huge increase, by a factor of about 100, in the rate coefficient for ammonia ligation upon the addition of a c-C_5H_5 ligand to Mg^+ and Fe^+ can qualitatively be attributed to the sharp increase in the number of degrees of freedom in the transient intermediate (c-C_5H_5)$M(NH_3)^+$*. There is no indication from the CID profiles that the M^+-NH_3 binding enthalpies are significantly enhanced by the presence of the c-C_5H_5 ligand.

In the case of the ligation of Mg^+, we propose that the precipitous drop in the rate of ligation for the addition of the fourth ligand and the apparent emergence of a weakly bonded

TABLE 6: Calculated Standard Enthalpies of Formation, $\Delta H^\circ_{f,298}$ in kcal mol^{-1} at 298 K

	standard enthalpies of formation		
ion	B3LYP/ 6-31+G(d)	B3LYP/ 6-311++G(2df,p)	MP4SDTQ(fc)/ 6-311++G(2df,p)
I	167.1	163.6	164.5
III	131.5	125.1	126.5
V	103.1	93.5	
VII	81.0		

population of ligated ions in the CID spectra for $Mg(NH_3)_3^+$ and $Mg(NH_3)_4^+$ may signify *a change in the nature of the bonding* with the addition of the third ligand. The addition of the fourth ammonia and a fraction of the addition of a third ammonia could lead to hydrogen-bond formation with one of the ammonia ligands already attached to Mg^+ and so begin a second coordination shell rather than bond directly to the magnesium. Outer-shell ligation by hydrogen bonding may become preferred simply on steric grounds. The inflection in the $Mg(NH_3)_3^+$ dissociation profile shown in Figure 1 is consistent with the presence of two isomers (isomers **V** and **VI** in Figure 6), and thus indicates a transition from stronger direct bonding with Mg^+ to weaker hydrogen bonding in an outer solvation shell. The correlation shown in Figure 7 of measured onset energies for multicollision-induced dissociation with computed Mg^+-NH_3 and hydrogen-bond energies provides further support for such a transition. The two onset voltages ascribed to desolvation correlate nicely with the computed hydrogen-bond energies. Also, it should be noted that addition of a fourth ammonia ligand to the hydrogen-bonded isomer of $Mg(NH_3)_3^+$ may lead to a doubly coordinated, doubly hydrogen-bonded isomer, not shown in Figure 6 and not calculated, in addition to isomer **VIII**.

The occurrence of a transition in the nature of the bonding of ammonia in the sequential ligation of $(c\text{-}C_5H_5)Mg^+$ and $(c\text{-}C_5H_5)Fe^+$ is less clear. Since ligation enthalpies were not calculated for these systems, it was not possible to pursue a correlation of the type shown in Figure 7 for the ammonia ligation of Mg^+. However, it is worthy of note that the CID profile of $(c\text{-}C_5H_5)Mg(NH_3)_3^+$ also shows two populations (see Figure 4) that again would be consistent with the occurrence of hydrogen bonding of the third ammonia ligand in a fraction of the $(c\text{-}C_5H_5)Mg(NH_3)_3^+$ ions. The CID profiles in Figure 2 show no evidence for the presence of two isomers of $Fe(NH_3)_3^+$. Our measured dissociation onset is low, but this is consistent with the low binding enthalpy for $Fe(NH_3)_2^+-NH_3$ reported recently by Walter and Armentrout.[7] It is not inconceivable, however, that the third ligand in $Fe(NH_3)_3^+$ and the third and fourth ligands in $Fe(NH_3)_4^+$ are hydrogen-bonded rather than coordinated directly to Fe^+ in our experiments and even in those of Walter and Armentrout.[7] The low binding energies reported by Walter and Armentrout for $Fe(NH_3)_2^+-NH_3$ and $Fe(NH_3)_3^+-NH_3$ lie in an energy realm possible for hydrogen bonding.

Conclusion

The atomic metal ions Mg^+ and Fe^+ and the organometallic ions $(c\text{-}C_5H_5)Mg^+$ and $(c\text{-}C_5H_5)Fe^+$ can be ligated sequentially with ammonia in the gas phase at room temperature in helium buffer gas at 0.35 Torr. The rate coefficient for ligation was observed to depend on the extent of ligation. In the case of the ligation of Mg^+ and Fe^+ the rate coefficient is largest for the second addition of ammonia. The presence of the cyclopentadienyl substituent substantially enhances the primary rate of ligation with ammonia.

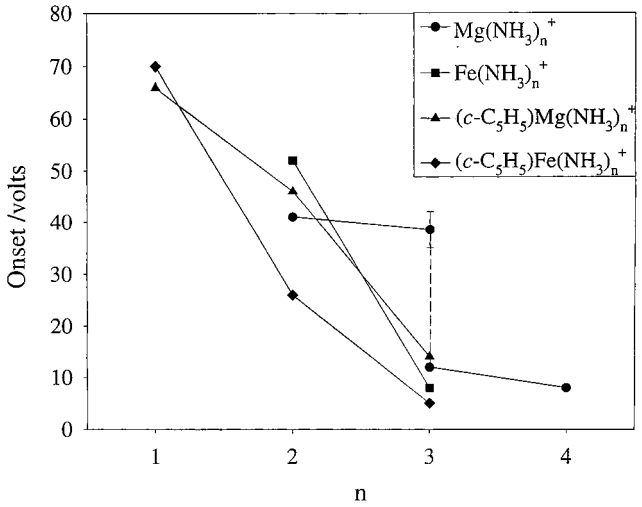

Figure 8. Correlation of the measured onset voltage for multicollision-induced dissociation with the number of ammonia ligands *n*. The break in the $Mg(NH_3)_n^+$ curve is consistent with a transition from stronger direct bonding to Mg^+ to weaker hydrogen bonding in an outer solvation shell. Two onsets were identified for the removal of the third ammonia molecule, one being an upper limit.

TABLE 7: Binding Enthalpies (in kcal mol^{-1}) at 298 K Reported for $Fe^+(NH_3)_{n-1}-NH_3$

$n=1$	$n=2$	$n=3$	$n=4$	ref
38.5 ± 4	48.7 ± 4			Marinelli (1989)[6]
43.0 ± 3[a]	50.7 ± 3[a]			Langhoff et al. (1991)[8]
44.0 ± 2.9	54.3 ± 2.6	16.5 (±3.6)	10.5 (±1.7)	Walter and Armentrout (1998)[7]

[a] Theoretical results of Langhoff et al. converted to 298 K (ref 8).

Multicollision-induced dissociation experiments indicate a lower threshold for dissociation of the more highly ligated ions of $Mg(NH_3)_n^+$, $Fe(NH_3)_n^+$, $(c\text{-}C_5H_5)Mg(NH_3)_n^+$, and $(c\text{-}C_5H_5)Fe(NH_3)_n^+$ and a uniquely high stability for $Fe(NH_3)_2^+$. In the case of the dissociation of $Mg(NH_3)_n^+$ the observed thresholds for dissociation correlate with computed bond dissociation energies. Computations reveal the existence of stable $Mg(NH_3)_n^+$ structures involving either direct Mg−N bonding through the lone pair on the nitrogen to the magnesium or hydrogen bonding in an "outer" solvation shell. Mg−N binding energies range from 41.4 to 15.5 kcal mol^{-1} for the direct addition of up to four ammonia molecules and from 16.0 to 10.4 kcal mol^{-1} for hydrogen bonding. Magnesium insertion, although possible, is not the best geometry on the $MgNH_3^+$ surface. Calculations of Mg−N bond lengths show that $Mg(NH_3)_n^+$ "inflates" with increasing ammonia addition as the Mg−N bond lengths increase with increasing ammonia addition until the addition of the fourth ammonia that triggers the formation of a tighter tetrahedral structure.

A two-step mechanism, involving the formation and collisional stabilization of a ligated transient intermediate, can account qualitatively for the observed trends in the magnitude of the rate coefficient with increasing ligation. In the case of the sequential ligation of Mg^+ for which computed binding energies are available, the two-step mechanism also provides an interpretation of the observed precipitous drop in the rate of ligation of the fourth ligand in terms of a change in the nature of the bonding from direct Mg^+-NH_3 bonding to outer-shell N−H···N hydrogen bonding. Additional support for this

hypothesis is found in a correlation of measured onset energies for multicollision-induced dissociation with computed Mg^+-NH_3 and hydrogen-bond energies and in the observed variation in the measured onset energy with the number of ligands added.

Acknowledgment. We thank Steve Quan and Alwin Cunje for technical assistance in the calculations. Continued financial support to A.C.H. and D.K.B. from the Natural Science and Engineering Research Council of Canada is greatly appreciated.

References and Notes

(1) See, for example, the following. (a) Eller, K.; Schwarz, H. *Chem. Rev.* **1991**, *91*, 1121. (b) Armentrout, P. B. In *Selective Hydrocarbon Activation: Principles and Progress*; Davies, J. A., Watson, P. L., Liebman, J. F., Greenberg, A., Eds.; VCH: New York, 1990; pp 467−533. (c) Weisshaar, J. C. *Acc. Chem. Res.* **1993**, *26*, 213. (d) Armentrout, P. B.; Kickel, B. L. In *Organometallic Ion Chemistry*; Freiser, B. S., Ed.; Kluwer Academic: Dordrecht, 1996; pp 1−45.

(2) (a) Baranov, V.; Javahery, G.; Hopkinson, A. C.; Bohme, D. K. *J. Am. Chem. Soc.* **1995**, *117*, 12801. (b) Baranov, V.; Javahery, G.; Bohme, D. K. *Chem. Phys. Lett.* **1995**, *239*, 339. (c) Baranov, V.; Bohme, D. K. *Int. J. Mass Spectrom. Ion Phys.* **1995**, *149*/*150*, 259. (d) Baranov, V.; Becker, H.; Bohme, D. K. *J. Phys. Chem. A* **1997**, *101*, 5137.

(3) See, for example, the following. Tonkyn, R.; Ronan, M.; Weisshaar, J. C. *J. Phys. Chem.* **1988**, *92*, 92.

(4) Bauschlicher, C. W.; Sodupe, M.; Partridge, H. *J. Chem. Phys.* **1992**, *96*, 4453.

(5) Bauschlicher, C. W.; Partridge, H. *Chem. Phys. Lett.* **1991**, *181*, 129.

(6) Marinelli, P. J.; Squires, R. R. *J. Am. Chem. Soc.* **1989**, *111*, 4103.

(7) Walter, D.; Armentrout, P. B. *J. Am. Chem. Soc.* **1998**, *120*, 3176.

(8) Langhoff, S. R.; Bauschlicher, C. W.; Partridge, H.; Sodupe, M. *J. Phys. Chem.* **1991**, *95*, 10677.

(9) Weinheimer, C. J.; Lisy, J. M. *Int. J. Mass Spectrom. Ion Processes* **1996**, *159*, 197.

(10) (a) MacKay, G. J.; Vlachos, G. D.; Bohme, D. K.; Schiff, H. I. *Int. J. Mass Spectrom. Ion Phys.* **1988**, *36*, 259. (b) Raksit, A. B.; Bohme, D. K. *Int. J. Mass Spectrom. Ion Phys.* **1983**, *55*, 69.

(11) Baranov, V. I.; Bohme, D. K. *Int. J. Mass Spectrom. Ion Proc.* **1996**, *154*, 71.

(12) Frisch, M. J.; Trucks, G. W.; Schlegel, H. B.; Gill, P. M. W.; Johnson, B. G.; Robb, M. A.; Cheeseman, J. R.; Keith, T.; Petersson, G. A.; Montgomery, J. A.; Raghavachari, K.; Al-Laham, M. A.; Zakrzewski, V. G.; Ortiz, J. V.; Foresman, J. B.; Cioslowski, J.; Stefanov, B. B.; Nanayakkara, A.; Challacombe, M.; Peng, C. Y.; Ayala, P. Y.; Chen, W.; Wong, M. W.; Andres, J. L.; Reploge, E. S.; Gomperts, R.; Martin, R. L.; Fox, D. J.; Binkley, J. S.; DeFrees, D. J.; Baker, J.; Stewart, J. P.; Head-Gordon, M.; Gonzalez, C.; Pople, J. A. *GAUSSIAN 94*, revision B.2; Gaussian, Inc.: Pittsburgh, PA, 1995.

(13) (a) Hohenburg, P.; Kohn, W. *Phys. Rev. B* **1964**, *136*, 864. (b) Kohn, W.; Sham, L. J. *Phys. Rev. A* **1965**, *140*, 1133. (c) Salahub, D. R.; Zerner, M. C. *The Challenge of d and f Electrons*; American Chemical Society: Washington, DC, 1989. (d) Parr, R. G.; Yang, W. *Density Functional Theory of Atoms and Molecules*; Oxford University Press: Oxford, U.K., 1989. (e) Perdew, J. P.; Wang, Y. *Phys. Rev. B* **1992**, *45*, 244. (f) Perdew, J. P.; Chevery, J. A.; Vosko, S. H.; Jackson, K. A.; Pederson, M. R.; Singh, D. J.; Fiolhais, C. *Phys. Rev. B* **1992**, *46*, 6671. (g) Labanowski, J. K.; Andzelm, J. W. *Density Functional Methods in Chemistry*; Springer-Verlag: New York, 1991. (h) Sosa, C.; Lee, C. *J. Chem. Phys.* **1993**, *98*, 8004. (i) Andzelm, J.; Wimmer, E. J. *Chem. Phys.* **1992**, *96*, 1280. (j) Scuseria, G. E. *J. Chem. Phys.* **1992**, *97*, 7528. (k) Becke, A. D. *J. Chem. Phys*. **1992**, *97*, 9173. (l) Becke, A. D. *J. Chem. Phys*. **1992**, *96*, 2155. (m) Gill, P. M. W.; Johnson, B. G.; Pople, J. A.; Frisch, M. J. *Chem. Phys. Lett.* **1992**, *197*, 499. (n) Stephens, P. J.; Devlin, F. J.; Chabalowski, C. F.; Frisch, M. J. *J. Phys. Chem.* **1994**, *98*, 11623. (o) Becke, A. D. Density-functional Thermochemistry. III. The Role of the Exact Exchange. *J. Chem. Phys*. **1993**, *98*, 5648.

(14) Slater, J. C. *Quantum Theory of Molecules and Solids. Vol. 4: The Self-Consistent Field for Molecules and Solids*; McGraw-Hill: New York, 1974.

(15) Becke, A. D. *Phys. Rev. A* **1988**, *38*, 3098.

(16) Lee, C.; Yang, W.; Parr, R. G. *Phys. Rev. B* **1988**, *37*, 785.

(17) Miehlich, B.; Savin, A.; Stoll, H.; Preuss, H. *Chem. Phys. Lett.* **1989**, *157*, 200.

(18) Møller, C.; Plesset, M. S. *Phys. Rev.* **1934**, *45*, 618.

(19) Su, T.; Bowers, M. T. *Int. J. Mass Spectrom. Ion Phys.* **1973**, *12*, 347.

(20) Linder, C. B.; Dalton, A. L.; Babcock, L. M. Glow Discharge Studies of Gas Phase Metal Ions: Reactions of Mg^+. In Proceedings of the 43rd ASMS Conference on Mass Spectrometry and Allied Topics, Atlanta, GA, May 21−26, 1995.

(21) (a) Rodriquez, C. F.; Hopkinson, A. C. *J. Phys. Chem.* **1993**, *97*, 849. (b) Rodriquez, C. F.; Hopkinson, A. C. *J. Org. Chem*. **1992**, *57*, 4869. (c) Rodriquez, C. F.; Bohme, D. K.; Hopkinson, A. C. *J. Org. Chem*. **1993**, *58*, 3344.

(22) (a) Rodriquez, C. F.; Sirois, S.; Hopkinson, A. C. *J. Org. Chem.* **1992**, *57*, 4869. (b) Rodriquez, C. F.; Bohme, D. K.; Hopkinson, A. C. *J. Phys. Chem.* **1996**, *100*, 2942.

(23) Good, A. *Trans. Faraday Soc*. **1971**, *67*, 3495.